nature climate change

LETTERS

PUBLISHED ONLINE: 21 NOVEMBER 2016 | DOI: 10.1038/NCLIMATE3158

Greenhouse gas emissions intensity of global croplands

Kimberly M. Carlson[1,2*], James S. Gerber[1], Nathaniel D. Mueller[3,4], Mario Herrero[5], Graham K. MacDonald[1,6], Kate A. Brauman[1], Petr Havlik[7], Christine S. O'Connell[1,8], Justin A. Johnson[1], Sassan Saatchi[9] and Paul C. West[1]

Stabilizing greenhouse gas (GHG) emissions from croplands as agricultural demand grows is a critical component of climate change mitigation[1–3]. Emissions intensity metrics—including carbon dioxide equivalent emissions per kilocalorie produced ('production intensity')—can highlight regions, management practices, and crops as potential foci for mitigation[4–7]. Yet the spatial and crop-wise distribution of emissions intensity has been uncertain. Here, we develop global crop-specific circa 2000 estimates of GHG emissions and GHG intensity in high spatial detail, reporting the effects of rice paddy management, peatland draining, and nitrogen (N) fertilizer on CH_4, CO_2 and N_2O emissions. Global mean production intensity is 0.16 Mg CO_2e M kcal^{-1}, yet certain cropping practices contribute disproportionately to emissions. Peatland drainage (3.7 Mg CO_2e M kcal^{-1})—concentrated in Europe and Indonesia—accounts for 32% of these cropland emissions despite peatlands producing just 1.1% of total crop kilocalories. Methane emissions from rice (0.58 Mg CO_2e M kcal^{-1}), a crucial food staple supplying 15% of total crop kilocalories, contribute 48% of cropland emissions, with outsized production intensity in Vietnam. In contrast, N_2O emissions from N fertilizer application (0.033 Mg CO_2e M kcal^{-1}) generate only 20% of cropland emissions. We find that current total GHG emissions are largely unrelated to production intensity across crops and countries. Climate mitigation policies should therefore be directed to locations where crops have both high emissions and high intensities.

The food system, including crop and livestock production, is responsible for up to a third of total anthropogenic GHG emissions[8]. Land-use change, including cropland expansion into carbon-rich forests, was the dominant contributor to land-based emissions throughout the 1990s[9]. International agreements, national policies, and private sector commitments now focus on reducing emissions from such agricultural expansion[10]. From 2000–2010, global crop production growth (2% yr^{-1}) outpaced harvested area expansion (0.8% yr^{-1})[11]. During this time, expansion-related emissions stabilized while emissions from crop management grew by about 1% yr^{-1}; by 2010, agricultural production emissions were greater than land change emissions[12]. Since improving yields on existing croplands supports future food demand[13], GHG reduction strategies targeted to crop management practices are essential to address agriculture's contribution to climate change.

Field investigations and meta-analyses indicate that changing management practices can increase crop yields with negligible growth or even reductions in GHG emissions[4,5,14,15]. Assessing the total climate abatement potential of such changes requires first identifying emissions intensity associated with diverse farming systems. Although the accuracy and scope of national-scale cropland emissions estimates are improving, the geographic distribution of these emissions remains relatively uncertain. With some exceptions[16,17], most available global studies either report crop-specific emissions at the national level[11] or national to subnational emissions aggregated for many crops (Supplementary Discussion).

We advance spatially explicit global GHG emissions accounting by coupling biophysical models with novel 5-arc-minute resolution data on land surface attributes and crop harvest and management (Methods). We consider CH_4 emissions from paddy (flooded) rice cultivation, CO_2, N_2O and CH_4 flux from agricultural peatland draining, and direct and indirect N_2O emissions from synthetic N fertilizer and manure application. These fluxes account for the majority of GHG emissions from cropland agriculture[11], but exclude certain emissions sources (for example, energy for fertilizer manufacture, liming). Our approach provides a crop-specific subnational assessment of how agricultural management practices interact with biophysical characteristics to generate heterogeneous patterns of GHG emissions. We estimated emissions from 172 crops (Supplementary Data 1 and 2); here we focus on the ten food crops and world regions (nine countries plus Europe) that contribute the greatest total GHG emissions.

In 2000, we find total global cropland GHG emissions of 1994 $\pm$ 2172 Tg CO_2e (mean $\pm$ standard deviation), representing 4.5 $\pm$ 4.9% of anthropogenic emissions[18]. This estimate excludes emissions from the livestock sector, land-cover change, and pre- and post-production emissions. Largely due to an updated N_2O emissions model[16] and spatially explicit evaluation of peatlands under cultivation, our assessment suggests substantially lower total emissions than compiled assessments from comparable 2000-era studies, which range from 2294–3102 Tg CO_2e yr^{-1} (Supplementary Discussion). About 48% of our estimated emissions are from flooded rice, 32% from

[1]Institute on the Environment, University of Minnesota, Saint Paul, Minnesota 55108, USA. [2]Department of Natural Resources and Environmental Management, University of Hawai'i, Honolulu, Hawai'i 96822, USA. [3]Department of Earth and Planetary Sciences, Harvard University, Harvard, Massachusetts 02138, USA. [4]Department of Organismic and Evolutionary Biology, Harvard University, Harvard, Massachusetts 02138, USA. [5]Commonwealth Scientific and Industrial Research Organization (CSIRO), St Lucia, Queensland 4067, Australia. [6]Department of Geography, McGill University, Montreal, Quebec H3A 0B9, Canada. [7]Ecosystem Services and Management Program, International Institute for Applied Systems Analysis, Laxenburg, Austria. [8]Department of Environmental Science, Policy, and Management, University of California, Berkeley, California 94720, USA. [9]Jet Propulsion Laboratory, California Institute of Technology, Pasadena, California 91109, USA. *e-mail: kimcarlson@gmail.com

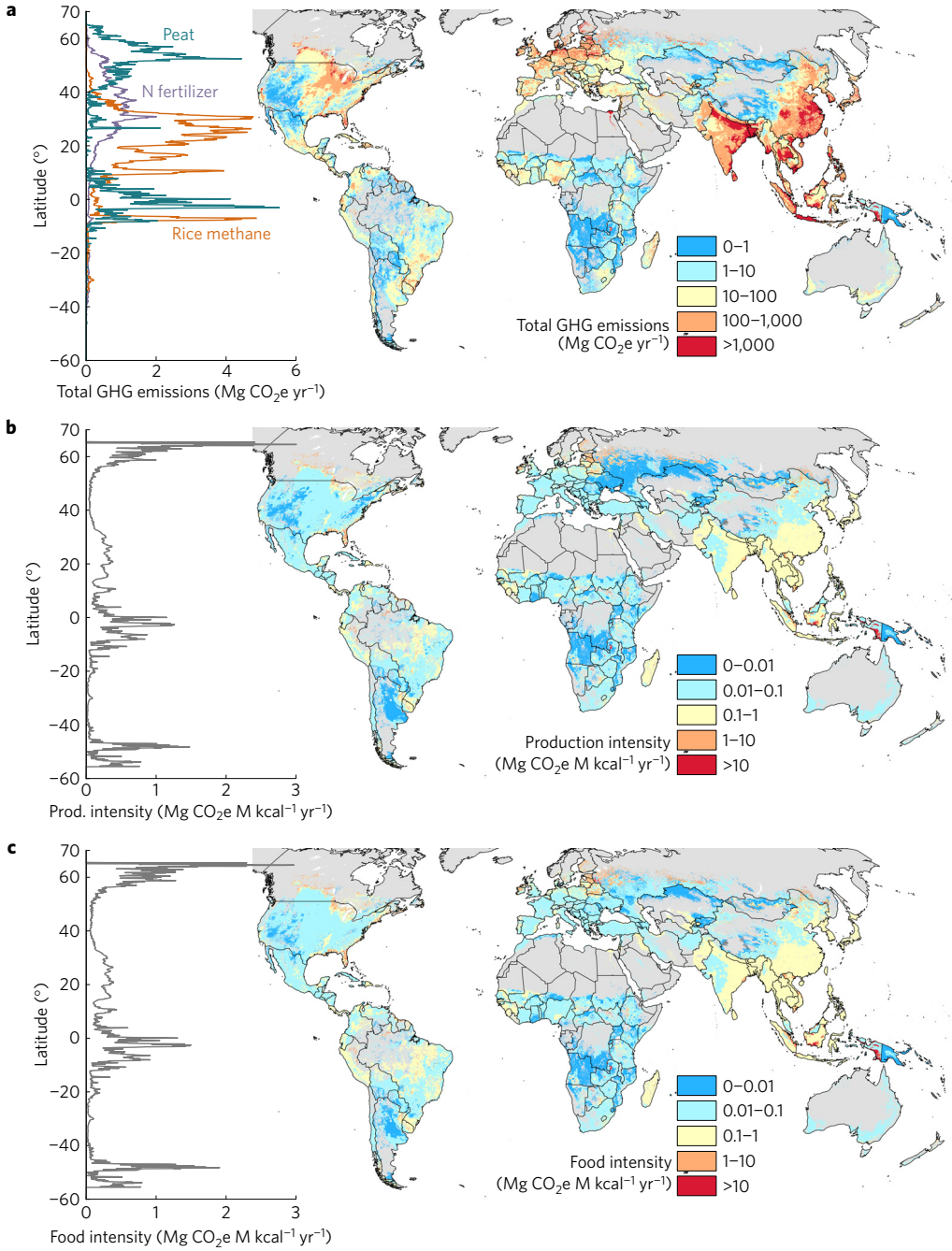

Figure 1 | Global distribution of circa 2000 greenhouse gas (GHG) emissions from 172 crops. Cropland GHGs consist of CH_4 from rice cultivation, CO_2, N_2O, and CH_4 from peatland draining, and N_2O from N fertilizer application. Total emissions from each grid cell (**a**) are concentrated in Asia, and are distinct from patterns of production intensity (**b**, all crop calories), and food intensity (**c**, excludes calories dedicated to industrial and non-food uses, and assumes that 12% of livestock feed calories are available in foods for human consumption[24]). Latitudinal plots represent total (**a**) and kilocalorie-weighted mean (**b**,**c**) quantities.

peatland cultivation, and 20% from N fertilizer application (Fig. 1 and Supplementary Fig. 1). The top ten crops account for 75% of GHG emissions (Fig. 2a). Total emissions are concentrated in Asia, with China, Indonesia and India contributing 51% of all emissions (Fig. 2f).

Rice is a staple for almost half the global population, and demand for rice is projected to increase substantially in coming years[19]. Rice paddy flooding leads to anaerobic decomposition and associated CH_4 flux. Using spatially resolved irrigation, organic amendment, and crop calendar data, we estimate that such flooding generates $962 \pm 2170\ Tg\ CO_2e$, or 92% of total rice emissions. Rice CH_4 emissions are concentrated in irrigated areas, which make up 60% of total rice harvested area but produce 78% of emissions. India produces 22% of global rice and is the leading emitter of rice CH_4, contributing 27% of the global total. China provides a third of all rice but just 23% of rice CH_4 emissions, due to mid-season paddy drainage practices that reduce CH_4 flux[14,20]. In contrast, continuous flooding and triple cropping in Vietnam's Mekong and Red River deltas drive 10% of global rice CH_4emissions, yet Vietnam produces just 5.0% of global rice. Our mean rice CH_4 emissions estimate represents 84–131% of recent global evaluations (Supplementary Discussion).

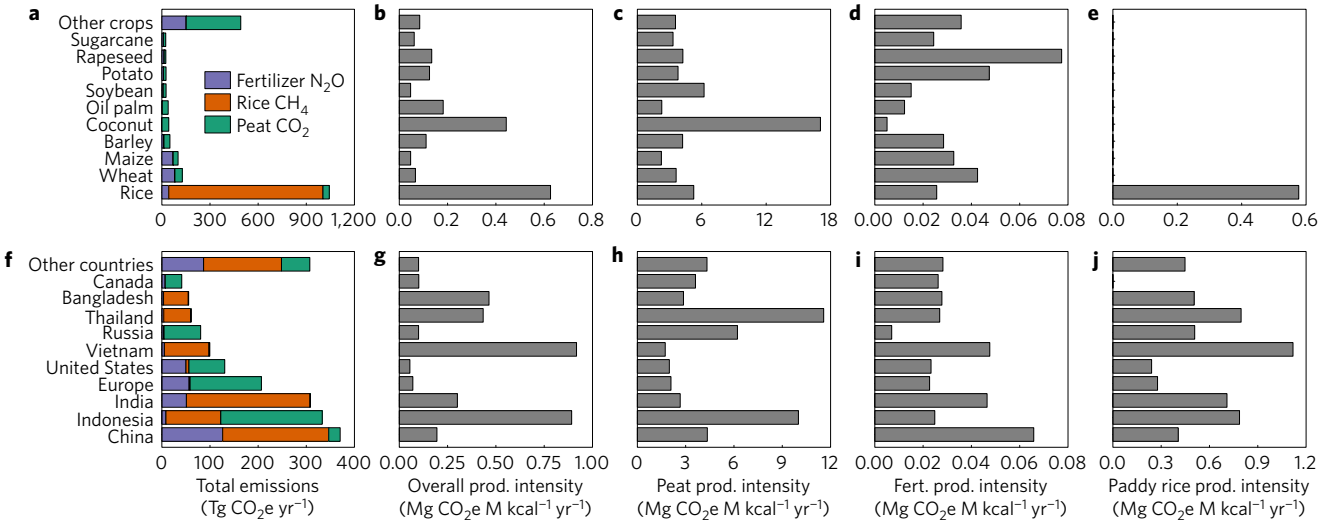

Figure 2 | Global cropland greenhouse gas emissions and intensities of the top ten emitting food crops and regions, and all other crops and regions. **a**–**e**, Analysis of emissions by crop. Rice accounts for 48% of total crop emissions (**a**) because of high CH_4 emissions associated with rice paddy flooding (**e**). Coconut has high overall production intensity (**b**) due to 2.2% its of harvested area located on peatlands (**c**). Fertilizer production intensity is elevated for rapeseed and potato (**d**). Oil palm's mean global annual caloric yields are 14-587% greater than other top crops, leading to low intensity across peat and fertilizer intensity metrics; substantial peat development (5.2% of harvested area) generates higher overall production intensity. **f**–**j**, Analysis of emissions by country. Total country emissions (**f**) are dominated by China, with extensive paddy rice and high fertilizer application rates. Vietnam's triple-cropped rice and Indonesia's peatland development generate high overall GHG production intensity (**g**). Peat production intensity (**h**) exceeds fertilizer (**i**) and rice (**j**) intensities. Production intensity includes all crop calories. Food intensity excludes industrial and non-food calories, and assumes that 12% of calories used as livestock feed are available in foods for human consumption[24].

Drainage exposes carbon-dense peatland soils to oxygen and generates disproportionately large and sustained net GHG emissions. Peatland emissions may exceed those from deforestation over long timescales, and draining is linked to land subsidence, amplified fire risk, and regionally altered hydrology[21]. We combined global gridded peatland locations with resolved maps in countries with extensive peat deposits to quantify the fraction of each grid cell occupied by peat, leading to an estimate of 3.4 M km^2 occupied by peatlands globally (Supplementary Fig. 2). If crops are planted on peatlands in proportion to grid cell peat area, 4% of global peatlands are cultivated and 0.9% of global crop area (0.7% of harvested area, which accounts for double cropping and excludes fallow lands) is on peat. The majority of cropped peatlands are in Europe and Indonesia (Supplementary Data 3), where 2% and 5% of crop harvested areas are on peat, respectively.

Using emissions factors from the Intergovernmental Panel on Climate Change (IPCC) Wetlands Supplement (Methods), we calculate that emissions from draining peatlands for agriculture are 630 $\pm$ 90 Tg CO_2e yr^{-1}, composed of CO_2 (89% in CO_2e), N_2O (11%) and CH_4 (<1%). We do not account for reduced CH_4 emissions as a result of draining, which may slightly overestimate peatland emissions. In part because combined soil and off-site tropical peat CO_2 emissions factors are 1.2–1.8 times those in temperate and boreal climates, Indonesia emits 33% of total global cropland peat CO_2e. Our global peat area is 76–87% of the extent reported in other studies (3.9–4.4 M km^2, Supplementary Discussion). These studies report overall peat disturbance levels of 12–13%, compared to our 4% estimate of peat draining for croplands. Consequently, our mean cropland peat emissions estimate is ~51–80% of similar assessments.

To assess direct N_2O emissions from soils, we applied an exponential emissions-response model that accounts for lower N_2O emissions from paddy rice[16]. We quantified indirect N_2O emissions from leaching and volatilization by applying the IPCC 2006 Guidelines for National GHG Inventories[20] (Methods). Total N_2O emissions of 403 $\pm$ 74 Tg CO_2e are associated with application of 79 Tg N yr^{-1} of synthetic fertilizer and 7.4 Tg N yr^{-1} from livestock manure. Indirect N_2O emissions constitute ~24% of total N_2O emissions. China contributes 31% of total fertilizer emissions, whereas wheat (20%) and maize (17%) dominate crop emissions. Our estimates are 61% of the Food and Agriculture Organization (FAO) estimate[11], which assumes slightly higher synthetic N application (81 Tg N yr^{-1}), greater manure N inputs (24 Tg N yr^{-1}), and a linear emissions factor of 1%, in contrast to a mean of 0.77% in our nonlinear model (Supplementary Discussion).

Metrics chosen to quantify the environmental intensity of agriculture reflect priorities for policy and land management[22]. Considering emissions from crop production available for human consumption offers insight into potential synergies and frictions between food security and climate mitigation[23]. We estimate cropland GHG emissions intensity (Mg CO_2e M $kcal^{-1}$) based on total emissions per total kilocalorie production ('production intensity'), and emissions from food production per kilocalorie available as food ('food intensity')[24]. To calculate food calories, we excluded calories used for industrial or other non-food uses, and assumed that 12% of calories used as livestock feed were available in foods for human consumption[24].

Globally, mean cropland production intensity is 0.16 $\pm$ 0.23 Mg CO_2e M $kcal^{-1}$ (Fig. 1b), whereas food intensity averages 0.25 $\pm$ 0.31 Mg CO_2e M $kcal^{-1}$ (Fig. 1c). Crops used mostly for food (for example, rice; many vegetables and fruits) tend to have high production intensity, whereas crops with greater non-food uses (for example, maize and many oil crops) are associated with lower production intensity (Supplementary Fig. 3). These disparities suggest potential conflicts between climate and food security goals. Switching among crops based on their production intensities could reduce the overall emissions intensity of croplands, but this could alter dietary diversity and the nutritional value of food[24,25]. This tension is especially great for rice, with 83% of production available as food, while being the most GHG intensive major crop (0.63 Mg CO_2e M $kcal^{-1}$ production intensity and 0.71 Mg CO_2e M $kcal^{-1}$ food intensity, Fig. 2e).

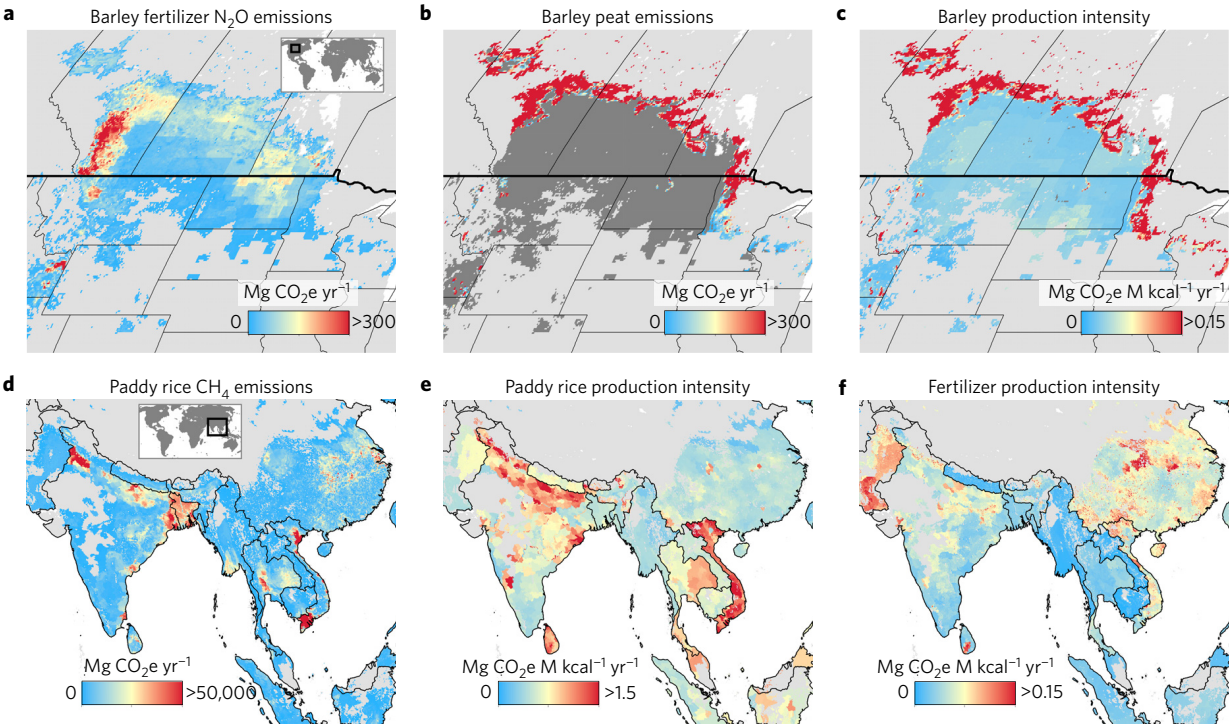

Figure 3 | Regional variation in cropland greenhouse gas emissions and intensities. a–c, North America. Total barley emissions per grid cell from fertilizer N_2O (**a**) and from peatland drainage (**b**) are concentrated in Canada. Grey indicates locations with barley production but no peat. Barley production intensity (**c**) is greatest on peatlands. However, in regions without peat, production intensity patterns are distinct from total emissions. **d–f**, Asia. Total rice CH_4 emissions per grid cell are highest in Vietnam's Mekong and Red River deltas (**d**) but are are largely unrelated to rice CH_4 production intensity (**e**). Fertilizer N_2O production intensity (**f**) for all crops in rice-growing regions is less than rice CH_4 production intensity.

Total GHG emissions are a poor predictor of production intensity for both crops and countries (Supplementary Fig. 4). For instance, Vietnam is the sixth largest emitter yet has the highest production intensity (Fig. 2). Targeting mitigation efforts to crops and locations with high intensities and high emissions is therefore likely to be a more effective strategy than focusing solely on large emitters[26]. Our global-scale, spatially explicit, crop-specific GHG emissions assessment aims to provide consistent metrics that are relevant across scales and useful for identifying these areas. For example, we find considerable subnational heterogeneity of barley emissions in North America and rice emissions in mainland Asia (Fig. 3).

Global mean nitrogen-use efficiency is <50%, with high potential for efficiency gains[26,27]. Yet, nitrogenous fertilizer application is the least GHG intensive and most malleable of the management practices considered here, and is also directly linked to increasing yields[28]. By simulating N-driven increases in productivity for nine crops across low-yielding areas, we examined tradeoffs between calorie production and GHG emissions. We developed a scenario in which we applied a target yield of 75% of attainable rainfed yield to all croplands (rainfed and irrigated), thereby avoiding implicit requirements for additional irrigation infrastructure. To estimate N additions needed to achieve target yields, we used nitrogen-yield curves and rainfed maximum yields for crop-specific climate zones[28].

We estimate that targeted application of additional N fertilizer could produce 12.2% more total calories from the nine study crops compared to year 2000 production (Fig. 4). Such intensification might generate 12.4% extra fertilizer N_2O emissions, marginally elevating overall fertilizer production intensity (0.18%). Nitrogen fertilization to close yield gaps may increase or reduce the emissions intensity of croplands, and this change depends on the crop- and climate-specific yield response[28] as well as the distribution of N application rates, with higher rates driving relatively greater emissions increases[16].

Although our model suggests that rice CH_4 emissions increase by 1.2% due to additional straw biomass inputs associated with higher yields, N fertilizer has complex effects on CH_4 emissions[29], and the amount of straw incorporated by farmers may be unrelated to total straw production. These uncertainties underscore the need to consider net lifecycle climate impacts from changes to cropping practices. For instance, paddy field aeration is recommended to reduce CH_4 emissions and maintain yields[14,20], but net soil CO_2 and N_2O emissions may increase with draining[6]. Full accounting of emissions intensity requires incorporation of additional on-farm dynamics (for example, tradeoffs between different GHGs) and off-farm processes (for example, emissions from fertilizer manufacture).

Reconciling rapidly increasing crop demand with the pressing need to address global climate change by stabilizing or reducing emissions from agriculture is a complex problem requiring novel policy measures to incentivize best practices[10]. Our spatially refined cropland GHG emission data can inform such interventions, which may include farmer education through extension and outreach, corporate sustainability commitments, national food policies, and multilateral agreements. Locally valid approaches are critical for application to specific regions[30]. Producers require support to better manage additional N inputs for nitrogen-use efficiency, and to implement agro-ecological techniques that lessen input dependence[5,10,27]. Our findings clearly indicate that climate mitigation policies for croplands should prioritize elimination of peatland draining. Future research evaluating tradeoffs between GHG emissions and food security should consider not only food production, but also the nutritional value of food[23]. Such strategies have great near-term potential to reduce the GHG emissions intensity of global agriculture.

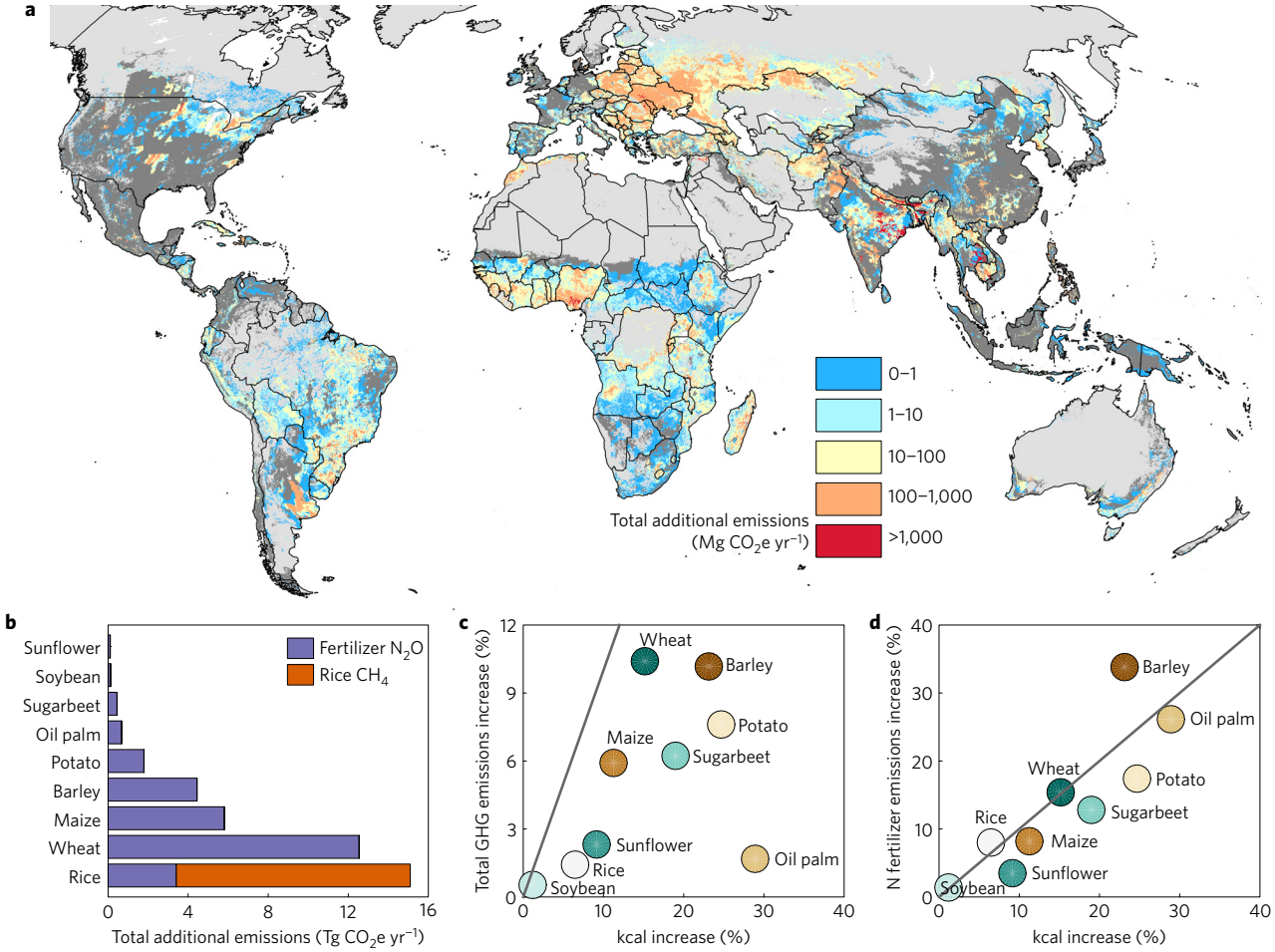

Figure 4 | Increased kilocalorie production relative to cropland greenhouse gas (GHG) emissions under an intensification scenario that relies on additional fertilizer application to close yield gaps for nine crops. a, Total additional GHG emissions per grid cell from intensification. Dark grey denotes locations of 2000-era croplands with no emissions increase, either due to no additional fertilizer inputs, or absence of one of the focal crops. **b**, Additional emissions relative to 2000-era, showing that increasing energetic production by 12% through fertilizer additions generates 2.9% greater total GHG emissions. **c**, Relative additional GHG emission versus kilocalorie production varies among crops, but energetic production always outpaces emissions. **d**, Additional N_2O emissions are relatively less than additional kilocaloric production for crops except barley, rice, soybean, and wheat. Grey line denotes 1:1 ratio between relative additional kilocaloric and GHG emission increases over the 2000-era.

Methods

Methods and any associated references are available in the online version of the paper.

Received 25 January 2016; accepted 22 September 2016; published online 21 November 2016

References

1. Foley, J. A. *et al*. Solutions for a cultivated plane. *Nature* **478,** 337–342 (2011).
2. Lipper, L. *et al*. Climate-smart agriculture for food security. *Nat. Clim. Change* **4,** 1068–1072 (2014).
3. Tilman, D., Balzer, C., Hill, J. & Befort, B. L. Global food demand and the sustainable intensification of agriculture. *Proc. Natl Acad. Sci. USA* **108,** 20260–20264 (2011).
4. Grassini, P. & Cassman, K. G. High-yield maize with large net energy yield and small global warming intensity. *Proc. Natl Acad. Sci. USA* **109,** 1074–1079 (2012).
5. Van Groenigen, J. W., Velthof, G. L., Oenema, O., Van Groenigen, K. J. & Van Kessel, C. Towards an agronomic assessment of N_2O emissions: a case study for arable crops. *Eur. J. Soil Sci.* **61,** 903–913 (2010).
6. Linquist, B, van Groenigen, K. J., Adviento-Borbe, M. A., Pittelkow, C. & van Kessel, C. An agronomic assessment of greenhouse gas emissions from major cereal crops. *Glob. Change Biol.* **18,** 194–209 (2012).
7. West, P. C. *et al*. Trading carbon for food: Global comparison of carbon stocks vs. crop yields on agricultural land. *Proc. Natl Acad. Sci. USA* **107,** 19645–19648 (2010).
8. Vermeulen, S. J., Campbell, B. M. & Ingram, J. S. I. Climate change and food systems. *Ann. Rev. Environ. Resour.* **37,** 195–222 (2012).
9. Houghton, R. A. *et al*. Carbon emissions from land use and land-cover change. *Biogeosciences* **9,** 5125–5142 (2012).
10. Godfray, H. C. J., Pretty, J., Thomas, S. M., Warham, E. J. & Beddington, J. R. Linking policy on climate and food. *Science* **331,** 1013–1014 (2011).
11. *FAOSTAT Online Statistical Service* (Food and Agriculture Organization (FAO), 2016); http://faostat3.fao.org
12. Tubiello, F. N. *et al*. The contribution of agriculture, forestry and other land use activities to global warming, 1990–2012. *Glob. Change Biol.* **21,** 2655–2660 (2015).
13. Garnett, T. *et al*. Sustainable intensification in agriculture: premises and policies. *Science* **341,** 33–34 (2013).
14. Feng, J. F. *et al*. Impacts of cropping practices on yield-scaled greenhouse gas emissions from rice fields in China: A meta-analysis. *Agr. Ecosyst. Environ.* **164,** 220–228 (2013).
15. Chen, X. *et al*. Producing more grain with lower environmental costs. *Nature* **514,** 486–489 (2014).
16. Gerber, J. S. *et al*. Spatially explicit estimates of N_2O emissions from croplands suggest climate mitigation opportunities from improved fertilizer management. *Glob. Change Biol.* **22,** 3383–3394 (2016).
17. Yan, X. Y., Akiyama, H., Yagi, K. & Akimoto, H. Global estimations of the inventory and mitigation potential of methane emissions from rice cultivation conducted using the 2006 Intergovernmental Panel on Climate Change Guidelines. *Glob. Biogeochem. Cycles* **23,** GB2002 (2009).
18. IPCC: Summary for policymakers. In *Climate Change 2007: The Physical Science Basis* (eds Solomon, S. *et al*.) (Cambridge Univ. Press, 2007).

19. Mohanty, S. Trends in global rice consumption. *Rice Today* **12,** 44–45 (2013).
20. IPCC, *2006 IPCC Guidelines for National Greenhouse Gas Inventories. Prepared by the National Greenhouse Gas Inventories Programme* (eds Eggleston, H. S., Buendia, L., Miwa, K., Ngara, T. & Tanabe, K.) (Institute for Global Environmental Strategies, 2006).
21. Frolking, S. *et al*. Peatlands in the Earth's 21st century climate system. *Environ. Rev.* **19,** 371–396 (2011).
22. Davis, S. J., Burney, J. A., Pongratz, J. & Caldeira, K. Methods for attributing land-use emissions to products. *Carbon Manage.* **5,** 233–245 (2014).
23. DeFries, R. *et al*. Global nutrition. Metrics for land-scarce agriculture. *Science* **349,** 238–240 (2015).
24. Cassidy, E. S., West, P. C., Gerber, J. S. & Foley, J. A. Redefining agricultural yields: from tonnes to people nourished per hectare. *Environ. Res. Lett.* **8,** 034015 (2013).
25. Khoury, C. K. *et al*. Increasing homogeneity in global food supplies and the implications for food security. *Proc. Natl Acad. Sci. USA* **111,** 4001–4006 (2014).
26. West, P. C. *et al*. Leverage points for improving global food security and the environment. *Science* **345,** 325–328 (2014).
27. Zhang, X. *et al*. Managing nitrogen for sustainable development. *Nature* **528,** 51–59 (2015).
28. Mueller, N. D. *et al*. Closing yield gaps through nutrient and water management. *Nature* **490,** 254–257 (2012).
29. Pittelkow, C. M. *et al*. Yield-scaled global warming potential of annual nitrous oxide and methane emissions from continuously flooded rice in response to nitrogen input. *Agr. Ecosyst. Environ.* **177,** 10–20 (2013).
30. Merrigan, K. *et al*. Designing a sustainable diet. *Science* **350,** 165–166 (2015).

Acknowledgements

We thank J. Foley for conversations conceptualizing this project. P. Engstrom, H. Rodrigues, D. Makowski, M. Ogg, S. Seibert and J. van de Steeg assisted with methods and data development. The Gordon and Betty Moore Foundation provided primary research funding, with additional support from the University of Minnesota Institute on the Environment, USDA National Institute of Food and Agriculture Hatch project HAW01136-H, managed by the College of Tropical Agriculture and Human Resources (K.M.C.), USDA Agriculture and Food Research Initiative fellowship 2016-67012-25208 (N.D.M.), NSF Hydrological Sciences grant 1521210 (N.D.M.), and the Belmont Forum/FACCE-JPI-funded DEVIL project NE/M021327/1 (J.S.G., M.H. and P.C.W.). The funders had no role in study design, data collection and analysis, decision to publish, or preparation of the manuscript.

Author contributions

K.M.C., P.C.W. and J.S.G. conceived the project. K.M.C., J.S.G., N.D.M., M.H., P.H., G.K.M. and K.A.B. provided new data and/or methods. K.M.C. and J.S.G. carried out modelling and analysis. All authors participated in writing the manuscript.

Additional information

Supplementary information is available in the online version of the paper. Reprints and permissions information is available online at www.nature.com/reprints. Correspondence and requests for materials should be addressed to K.M.C.

Competing financial interests

The authors declare no competing financial interests.

Methods

We calculated greenhouse gas (GHG) emissions from global croplands circa year 2000 for 172 crops[31] (Supplementary Table 1). The Monfreda *et al.*[31] cropland maps used in our analysis were derived by distributing agricultural census data onto remotely sensed cropland locations at 5-arc-minute resolution[32] and represent 1997–2003 means of yields and harvested areas. We converted all GHGs to carbon dioxide equivalent (CO_2e) using IPCC AR5 100 year Global Warming Potential[33].

Manure application to croplands. We combined circa 2000, 5-arc-minute livestock manure maps with manure management data (Supplementary Data 4)[34,35] to compute the mass of manure (MA, kg yr^{-1}) and manure N (NA, kg yr^{-1}) applied to croplands[16]:

$$\mathrm{MA} = M \times F_{\mathrm{MS}} \times (1 - F_{\mathrm{MSO}}) - N \times F_{\mathrm{MS}} \times (1 - F_{\mathrm{MSO}}) \times F_{\mathrm{LossMS}} \quad (1)$$

$$\mathrm{NA} = N \times F_{\mathrm{MS}} \times (1 - F_{\mathrm{MSO}}) \times (1 - F_{\mathrm{LossMS}}) \quad (2)$$

Here M is total manure mass produced (kg yr^{-1}), N is total nitrogen produced (kg yr^{-1}), F_{MS} is the fraction of total manure managed, F_{MSO} is the fraction of managed manure destined to other uses, and F_{LossMS} is the fraction of managed manure N lost prior to application to croplands (for example, leaching).

We assumed that manure is applied only within the 5-arc-minute grid cell in which it was produced, and computed manure application rate (kg ha^{-1} yr^{-1}) by dividing MA and NA by crop harvested area[32] (Supplementary Fig. 5). Some regions have high livestock densities relative to cropland area, generating elevated cropland manure application rates. Therefore, we capped grid cell manure application at the 99th percentile of the global application rate. Manure was applied at equal rates to all crops within a grid cell, except legumes. For leguminous crops, we allowed manure application until total N applied (synthetic + manure) reached the 99th percentile of the global synthetic N application rate to the crop in question.

Paddy rice CH_4 emissions. Anaerobic decomposition in flooded rice fields produces CH_4, which is then emitted to the atmosphere, mainly by rice plant-mediated transport[36]. We calculated global CH_4 emissions from rice cultivation by adapting the IPCC Tier 1 method[17,20] (Supplementary Table 2).

Rice cropping systems. To estimate the irrigated fraction of total rice harvested area, we used the MIRCA2000 data set[37], which includes monthly irrigated and rainfed rice growing areas across 402 spatial units. This data set maximizes consistency with cropland data[32], and draws from FAO's AQUASTAT database[38]. Since national statistics and FAO estimates diverge considerably for some countries, MIRCA2000 sometimes indicates irrigated rice areas in regions where Monfreda *et al.*[31] does not contain rice, and vice versa. To overcome this issue, for each of MIRCA2000's spatial units we calculated the fraction of irrigated area compared to total area (irrigated + rainfed) and applied these fractions to the Monfreda *et al.*[31] data set.

Irrigated rice. Draining rice fields during the growing season may reduce CH_4 emissions while conserving water and potentially increasing yields[39]. In irrigated areas, we allocated harvested area into continuously and intermittently flooded fractions. Intermittently flooded fractions were divided into regions drained one (single drainage, with 40% reduction in emissions compared to continuous flooding) or more (multiple drainage, with 48% reduction in emissions compared to continuous flooding) times during rice cultivation[20]. We compiled country-specific data on the fraction of rice area under these drainage regimes for the top 12 rice CH_4-emitting countries according to the FAO[11], as well as countries reporting drainage practices in ALGAS[40] reports (Supplementary Table 3). If a report did not specify whether intermittent flooding was single or multiple drainage, we assumed multiple drainage. For the rest of the world, we applied the mean fraction from these top 12 countries, excluding China, Japan and South Korea in this calculation, since these countries practise relatively unique rice water management[41].

Although pre-cultivation water status is critical to rice CH_4 emissions[42], few data are available on empirical patterns of flooding prior to planting. Thus, we applied the method of Yan *et al.*[17] to determine pre-cultivation water regimes (Supplementary Table 4).

Rainfed and upland rice. For rainfed and upland rice, we divided the non-irrigated rice fraction derived from the MIRCA2000 data set[37] into upland and rainfed systems. Upland rice is not flooded, and does not produce significant CH_4 emissions. The IPCC further splits rainfed rice—which is flooded but depends solely on rainwater input—into regular (water level <50 cm during cropping season), drought-prone (drought periods each cropping season), and deepwater (water level >50 cm for significant period of time during cropping season) categories[20]. Although global data on such rice cropping systems are unavailable at present, the most comprehensive subnational data set of similar rice cropping patterns presents an assessment of rice cultivation types across monsoon Asia, excluding Japan, circa 1990[43]. The classification system includes upland rice, deepwater rice with >100 cm water depth, and two rainfed classes with shallow (0–30 cm) and intermediate (30–100 cm) depth. We converted these data to a 5-arc-minute raster, and then translated these rice-cultivated areas into IPCC non-irrigated rice categories. We assumed that intermediate depth, shallow depth, deepwater, and upland categories from Huke and Huke[43] are equivalent to regular rainfed, drought-prone, deepwater, and upland categories from IPCC, respectively. Although this generates some inconsistencies (for example, some of Huke and Huke[43] intermediate rainfed should be classified as deepwater under the IPCC system), the classification makes our analysis comparable to Yan *et al.*[17], who took the same approach. Moreover, rainfed rice emissions scaling factors differ by only ~0.06 (Supplementary Table 2); discerning between upland, irrigated, and rainfed rice is therefore more important than differentiating between rainfed types. In regions not covered by Huke and Huke[43], we applied mean proportions from regions for which data are available (Supplementary Table 5).

Rice organic amendment. Organic amendments enhance rice CH_4 emissions because these substances contain decomposable carbon[44]. The IPCC provides scaling factors ('conversion factors') for various organic amendments. Global data on compost and green manure incorporation rates into rice paddy are not available, hence we consider only straw incorporation and farmyard manure. Manure application to rice was computed as described above. Rice straw production was estimated using a logarithmic function relating straw yield (Mg ha^{-1}) to grain yield (Mg ha^{-1})[17]. Straw may be incorporated into soils, left on fields, burned in fields, or removed and used as animal feed or bioenergy[45]. In Asia, intensification of rice cropping resulting in higher straw yields but less time to manage rice straw between cultivation periods, as well as reduced use of rice residues for off-field applications, is leading to burning as a preferred method of disposal[46,47].

To estimate the proportion of rice straw incorporated into soils, we first derived the percentage of agricultural residues burned in fields and as biofuels from Yevich and Logan[48] for Asian countries except China, which we derived from Yan *et al.*[49] (56% left on field, Supplementary Table 6). For all other countries, we applied the weighted mean for Asia (excluding China and India) reported by Yevich and Logan[48] (45% left on field). For single- and double-cropped systems, we assumed that 70% of this unburned straw is incorporated into soils[17]. For triple cropping, extremely short intervals between harvest and planting may prevent residue decomposition and release of nutrients before establishment of the next crop[45]. Thus, for triple-cropped rice systems we assume only 10% of unburned straw is incorporated. For rice double and triple cropping, we used the IPCC conversion factors for straw incorporated shortly (<30 days) before cultivation; for single-cropping systems, we applied the conversion factor assuming straw was incorporated long (>30 days) before cultivation (Supplementary Fig. 6).

Rice growing season length. The IPCC method generates daily rice CH_4 emissions. To estimate annual emissions, we quantified rice growing season length (days crop^{-1}) and number of crops per year using MIRCA2000 crop calendars[37]. We assumed that a crop is cultivated for half of the starting and ending months, generating growing season lengths ranging from 87–194 days for rainfed rice, and 91–152 days for irrigated rice (Supplementary Fig. 7). Rainfed areas produce only one crop per year. Irrigated areas produce one (42% of irrigated harvested area), two (50%) or three (8.7%) crops per year.

Peatland drainage. We generated a peatland map based on the Harmonized World Soil Database (HWSD, 30-arc-second resolution)[50]. With the HWSD, we calculated the proportion of histosols (HS) in each cell, and summed these proportions to generate total per-pixel peatland area. In regions known to have extensive peatlands, we replaced or supplemented the HWSD with more resolved data (Supplementary Table 7). We defined peat as the surface layer of soil consisting of partially decomposed vegetation with thickness ≥30 cm and organic carbon content of ≥30%, typically classified as histosols in soil databases. We contacted authors to acquire original data; in cases when there was no reply, we digitized peatlands from published maps. These individual maps were converted to 30-arc-second raster data, mosaicked, and overlaid on the HWSD peatland map. In most cases, these maps were binary, and we assumed full peat coverage in areas identified as peatlands. Where available (for example, Canada), we used fractional peatland cover. The combined data set was scaled to 5 arc-minutes, yielding a global raster of proportional grid cell area occupied by peatlands (Supplementary Fig. 2). Peatland area in this data set totals 3.42 M km^2.

We compared our data set with recent country-level estimates of peat area[51,51,53,54]. Where our estimate of country-level peatland area was outside the range of available estimates, we scaled proportional peat area to better match these expert estimates. To do so, we calculated the proportional difference between our estimate and that of others, ranked by degree of attention given to individual countries in the order: Page *et al.*[52]; Joosten[54]; Lappalainen[53]; and Joosten[51]. We then iteratively increased or decreased the proportion of peatlands in all peat cells in the country of interest by this difference until our estimate fell within the range of expert estimates, or until all available peat cells were 100% peat. Although peatlands described in some countries (for example, Japan) are not present in our

maps, these omitted peatlands occupy <2% of total global peatland area, and their exclusion is unlikely to substantially alter results.

Peatland emissions. Draining peatlands for agriculture lowers the water table and exposes peat soil organic matter to oxygen, which typically leads to increased CO_2 and N_2O emissions and reduced CH_4 emissions from the soil surface[33]. Draining can also generate elevated fluvial carbon loss[33,55]. To assess GHG emissions from peatland draining, we applied emissions factors from the IPCC Wetlands Supplement[33] (Supplementary Table 8). We calculated emissions from actual crop area on peatlands, rather than crop harvested area (which excludes fallow lands but accounts for double cropping), because peatland emissions factors can be applied only to actual area drained. In regions with substantial fallow areas or multiple crops per year, peat harvested area diverges from peat crop area (Supplementary Data 3). Peatland N_2O emissions were considered to be additive to N fertilizer-related emissions. For rice planted on peatlands, we attributed all CH_4 emissions with our rice model, and assumed no CH_4 emissions from peatland drainage.

N_2O emissions from N fertilizer. We developed 5-arc-minute crop-specific estimates of direct and indirect N_2O emissions from synthetic N fertilizer and animal manure N application to croplands for the year 2000. We do not account for N inputs from atmospheric deposition onto croplands, crop residues, soil mineralization, and non-manure organic N additions. We used the sum of synthetic and manure N fertilizer application rates as model input. We assumed a maximum combined synthetic + manure N application rate of 700 kg N ha^{-1}. Manure N application was computed as described above. For synthetic fertilizer inputs we used a global spatial N fertilizer data set[28], which estimates crop-specific synthetic fertilizer application rates circa 2000 (1997–2003).

Direct N_2O emissions. Nitrous oxide is generated by microbial transformation of N in soils through nitrification and de-nitrification processes[56,57]. Since reactive N availability is a major control on soil N_2O fluxes, elevated N_2O emissions are associated with N fertilizer application[56,58,59].

Our N_2O emissions model[16] is an updated version of the NL-N-RR model by Philibert *et al.*[60], which relates N_2O emissions to N fertilizer application rate using an exponential model and random parameters. This model outperformed linear models and exponential models with fixed parameters[60]. The updated model applies a discount factor parameter to account for reduced N_2O emissions from flooded rice[20], and was developed from a more recent and larger data set of field experiments[61].

Indirect N_2O emissions. Indirect N_2O emissions are generated from N volatilization as NH_3 and NO_X and re-deposition onto land and water surfaces[58]. In addition, in locations where water input is greater than soil water holding capacity, NO_3 may be leached into groundwater and water bodies[62]. We computed indirect emissions following IPCC's 2006 GHG Guidelines for National GHG Inventories[20]. Model terms included synthetic N and manure N inputs, the fraction of these inputs volatized or leached, and the IPCC's default emissions factors (Supplementary Table 9).

To calculate the fraction of a grid cell where N is lost from leaching, we assumed that leaching occurs when irrigation is used or the difference between rainy season (RS) precipitation inputs ($Precip_{RS}$, mm $month_{RS}^{-1}$) and rainy season potential evapotranspiration (PE_{RS}, mm $month_{RS}^{-1}$) is greater than soil water holding capacity (SWHC, mm):

$$\left(\sum \mathrm{Precip}_{\mathrm{RS}} - \sum \mathrm{PE}_{\mathrm{RS}}\right) > \mathrm{SWHC} \quad (3)$$

Gridded monthly total precipitation (mm) and mean temperature (°C) were derived from Hijmans and colleagues[63]. We calculated monthly PE_{RS} using a modified Hargreaves method that accounts for temperature and solar radiation[64,65]. Soil water holding capacity was considered to be the difference between wilting and field capacity in the top one metre of soil, and was calculated from International Soil Reference and Information Centre (ISRIC) soil data[66]. We computed mean soil water capacity for each of five soil layers as the mean of each soil water capacity weighted by the proportion soil occurrence, then summed SWHC for all layers.

To determine the rainy season for each grid cell, we identified all months in which precipitation was >1/3 of precipitation in the wettest month. We summed precipitation and evapotranspiration (ET) over those months. By considering the entire rainy season, this approach accounts for the likelihood that soils in any given rainy season month are already near saturation due to precipitation in a previous month. Finally, we evaluated the difference between rainy season precipitation and ET (equation (3)); where this value exceeds soil capacity, grid cells are subject to leaching.

As with rice, we determined irrigated fraction of each crop in each grid cell from crop-specific irrigated area for 26 crops and crop types in MIRCA2000[67]. We combined rainy season excess and irrigated maps to generate a fractional leaching and runoff map.

Kilocalorie production and available food GHG emission intensities. We calculated total crop kilocalorie production from yields (tons ha^{-1}) and harvested areas (ha)[31], and crop energy conversion factors (kcal ton^{-1})[11,68]. Since some crop production is allocated to livestock feed and other non-food uses, not all harvested crop calories are available for human consumption[24]. We distinguished total calorie production from food available calories using the FAOSTAT Food Balance Sheets[11], which provide estimates of the total domestic supply and domestic use as food, food manufacturing, feed, seed, waste, and other use. We estimated the mean 1998 to 2002 fraction of total calories used for food by crop, country, and year (Supplementary Fig. 8). We converted these quantities to calories using country-specific calorie conversion factors. Seed, waste, and other use were categorized as non-food uses. We assumed that 12% of the calories used as livestock feed for each crop were available in foods for human consumption[24], while the remainder of feed crop calories were considered as non-food use. To partition calories from oilseeds and the domestic use 'food manufacturing' category to food or non-food uses, we followed an approach similar to Cassidy and colleagues[24]. Finally, using bilateral crop trade data[68], we linked imported crop use to producing-country calorie production. We disaggregated minor crops grouped in the Food Balance Sheets to 172 individual crops based on FAO classifications.

Intensification scenario. To assess emissions associated with increasing yields through elevated fertilizer application, we applied crop-specific yield models[28]. The growing area for each crop was divided into 100 equal-area bins ('climate bins') of similar annual precipitation and growing degree-days (GDDs), calculated based on a crop-specific baseline temperature[69], and models were estimated that relate yields within each climate bin to irrigation and nutrient inputs. Temperature and precipitation inputs were derived from the WorldClim data set[63]. We calculated intensified production of nine crops (barley, maize, oil palm, potato, rice, soybean, sugarbeet, sunflower and wheat) by increasing yields to 75% of the rainfed attainable yield of each climate bin. Rainfed attainable yields are either the 95th percentile yield of the climate bin or the statistically estimated rainfed maximum yield for a given climate bin[28]. By establishing a yield target below rainfed maximum yield, we enable intensification on both irrigated and rainfed croplands, but avoid assumptions about changing on-farm water management, including expansion of irrigation and improved use of rainwater[70]. Such changes depend on multiple factors beyond the scope of our models, including the availability of sustainable water supplies under changing climate and resources for investment in such infrastructure[70]. We then assessed additional GHG emissions and production generated from this intensification (Fig. 4 and Supplementary Data 5). Under intensification, we assumed that total manure inputs remained fixed.

Uncertainty estimation. To estimate uncertainty around mean values, we applied a Monte Carlo approach, in which values were randomly selected from distributions. We repeated the sampling procedure 200 times, and report the sample mean and standard deviation. For total emissions from all crops or within a region, the standard deviation was calculated as the square root of the sum of variances for individual crops or pixels. For emission rates (for example, Mg CO_2 M $kcal^{-1}$), we calculated mean and standard deviation from the means of 200 model runs for all crops, or the mean across all pixels with values in a region, weighted by harvested area, peat harvested area, food harvested area, peat food harvested area, kilocalories, peat kilocalories, food kilocalories, or peat food kilocalories, as appropriate. Further details are provided in Supplementary Methods.

References

31. Monfreda, C., Ramankutty, N. & Foley, J. A. Farming the planet: 2. Geographic distribution of crop areas, yields, physiological types, and net primary production in the year 2000. *Glob. Biogeochem. Cycles* **22,** GB1022 (2008).
32. Ramankutty, N., Evan, A. T., Monfreda, C. & Foley, J. A. Farming the planet: 1. Geographic distribution of global agricultural lands in the year 2000. *Glob. Biogeochem. Cycles* **22,** GB1003 (2008).
33. IPCC, *2013 Supplement to the 2006 IPCC Guidelines for National Greenhouse Gas Inventories: Wetlands* (eds Hiraishi, T. *et al.*) (IPCC, 2014).
34. Herrero, M. *et al*. Biomass use, production, feed efficiencies, and greenhouse gas emissions from global livestock systems. *Proc. Natl Acad. Sci. USA* **110,** 20888–20893 (2013).
35. Robinson, T. *et al*. *Global Livestock Production Systems* (FAO, International Livestock Research Institute (ILRI), 2011).
36. Xu, S. P., Jaffe, P. R. & Mauzerall, D. L. A process-based model for methane emission from flooded rice paddy systems. *Ecol. Model.* **205,** 475–491 (2007).
37. Portmann, F. T. *Global Estimation of Monthly Irrigated and Rainfed Crop Areas on a 5 Arc-minute Grid* PhD thesis, Univ. Frankfurt (2011).
38. *AQUASTAT* (FAO, 2015); www.fao.org/nr/water/aquastat/main/index.stm.

39. Li, C. S. *et al*. Reduced methane emissions from large-scale changes in water management of China's rice paddies during 1980–2000. *Geophys. Res. Lett.* **29,** 1972 (2002).
40. Asia Least-cost Greenhouse Gas Abatement Strategy (ALGAS) (Asian Development Bank, Global Environment Facility and United Nations Development Program, 1998).
41. Adhya, T. K., Linquist, B., Searchinger, T., Wassmann, R. & Yan, X. *Wetting and Drying: Reducing Greenhouse Gas Emissions and Saving Water from Rice Production* (World Resources Institute, 2014).
42. Yan, X. Y., Yagi, K., Akiyama, H. & Akimoto, H. Statistical analysis of the major variables controlling methane emission from rice fields. *Glob. Change Biol.* **11,** 1131–1141 (2005).
43. Huke, R. E. & Huke, E. H. *Rice Area by Type of Culture: South, Southeast, and East Asia, A Revised and Updated Data Base* (International Rice Research Institute, 1997).
44. Vandergon, H. A. C. D. & Neue, H. U. Influence of organic-matter incorporation on the methane emission from a wetland rice field. *Glob. Biogeochem. Cycles* **9,** 11–22 (1995).
45. Bijay-Singh, , Shan, Y. H., Johnson-Beebout, S. E., Yadvinder-Singh, & Buresh, R. J. Chapter 3 crop residue management for lowland rice-based cropping systems in Asia. *Adv. Agron.* **98,** 117–199 (2008).
46. Gupta, P. K. *et al*. Residue burning in rice-wheat cropping system: causes and implications. *Curr. Sci.* **87,** 1713–1717 (2004).
47. Ahmed, T., Ahmad, B. & Ahmad, W. Why do farmers burn rice residue? Examining farmers' choices in Punjab, Pakistan. *Land Use Policy* **47,** 448–458 (2015).
48. Yevich, R. & Logan, J. A. An assessment of biofuel use and burning of agricultural waste in the developing world. *Glob. Biogeochem. Cycles* **17,** 1095 (2003).
49. Yan, X. Y., Ohara, T. & Akimoto, H. Bottom-up estimate of biomass burning in mainland China. *Atmos. Environ.* **40,** 5262–5273 (2006).
50. *Harmonized World Soil Database* V 1.2 (FAO, IIASA, SRIC, ISSCAS and JRC, 2012); http://webarchive.iiasa.ac.at/Research/LUC/External-World-soil-database/HTML.
51. Joosten, H. *The Global Peatland CO_2 Picture: Peatland Status and Drainage Related Emissions in all Countries of the World 35* (Wetlands International, 2009).
52. Page, S. E., Rieley, J. O. & Banks, C. J. Global and regional importance of the tropical peatland carbon pool. *Glob. Change Biol.* **17,** 798–818 (2011).
53. Lappalainen, E. *Global Peat Resources* 359 (International Peat Society, 1996).
54. Joosten, H. *Wise Use of Mires and Peatlands* 304 (International Mire Conservation Group and International Peat Society, 2002).
55. Jauhiainen, J. & Silvennoinen, H. Diffusion GHG fluxes at tropical peatland drainage canal water surfaces. *Suo* **63,** 93–105 (2012).
56. Butterbach-Bahl, K., Baggs, E. M., Dannenmann, M., Kiese, R. & Zechmeister-Boltenstern, S. Nitrous oxide emissions from soils: how well do we understand the processes and their controls? *Phil. Trans. R. Soc.* **368,** 20130122 (2013).
57. Stehfest, E. & Bouwman, L. N_2O and NO emission from agricultural fields and soils under natural vegetation: summarizing available measurement data and modeling of global annual emissions. *Nutr. Cycl. Agroecosyst.* **74,** 207–228 (2006).
58. Mosier, A. *et al*. Closing the global N_2O budget: nitrous oxide emissions through the agricultural nitrogen cycle. *Nutr. Cycl. Agroecosyst.* **52,** 225–248 (1998).
59. Davidson, E. A. The contribution of manure and fertilizer nitrogen to atmospheric nitrous oxide since 1860. *Nat. Geosci.* **2,** 659–662 (2009).
60. Philibert, A., Loyce, C. & Makowski, D. Quantifying uncertainties in N_2O emission due to N fertilizer application in cultivated areas. *PLoS ONE* **7,** e50950 (2012).
61. Shcherbak, I., Millar, N. & Robertson, G. P. Global metaanalysis of the nonlinear response of soil nitrous oxide (N_2O) emissions to fertilizer nitrogen. *Proc. Natl Acad. Sci. USA* **111,** 9199–9204 (2014).
62. Sawamoto, T., Nakajima, Y., Kasuya, M., Tsuruta, H. & Yagi, K. Evaluation of emission factors for indirect N_2O emission due to nitrogen leaching in agro-ecosystems. *Geophys. Res. Lett.* **32,** L03403 (2005).
63. Hijmans, R. J., Cameron, S. E., Parra, J. L., Jones, P. G. & Jarvis, A. Very high resolution interpolated climate surfaces for global land areas. *Int J. Climatol.* **25,** 1965–1978 (2005).
64. Zomer, R. J., Trabucco, A., Bossio, D. A. & Verchot, L. V. Climate change mitigation: a spatial analysis of global land suitability for clean development mechanism afforestation and reforestation. *Agric. Ecosyst. Environ.* **126,** 67–80 (2008).
65. Zomer, R. *et al*. *Trees and Water: Smallholder Agroforestry on Irrigated Lands in Northern India* (International Water Management Institute, 2007).
66. Batjes, N. H. *ISRIC-WISE Derived Soil Properties on a 5 by 5 Arc-minutes Global Grid* V 1.2 52 (ISRIC, 2012).
67. Portmann, F. T., Siebert, S. & Döll, P. MIRCA200 - Global monthly irrigated and rainfed crop areas around the year 2000: A new high-resolution data set for agricultural and hydrological modeling. *Glob. Biogeochem. Cycles* **24,** GB1011 (2010).
68. MacDonald, G. K. *et al*. Rethinking agricultural trade relationships in an era of globalization. *BioScience* **65,** 275–289 (2015).
69. Licker, R. *et al*. Mind the gap: how do climate and agricultural management explain the 'yield gap' of croplands around the world? *Glob. Ecol. Biogeogr.* **19,** 769–782 (2010).
70. Jägermeyr, J. *et al*. Integrated crop water management might sustainably halve the global food gap. *Environ. Res. Lett.* **11,** 025002 (2016).